JOURNAL OF GUIDANCE, CONTROL, AND DYNAMICS
Vol. 25, No. 2, March–April 2002

Control of Chaotic Motion in a Dual-Spin Spacecraft with Nutational Damping

P. A. Meehan* and S. F. Asokanthan†
University of Queensland, Brisbane, Queensland 4072, Australia

Control of chaotic vibrations in a dual-spin spacecraft with an axial nutational damper is achieved using two techniques. The control methods are implemented on two realistic spacecraft parameter configurations that have been found to exhibit chaotic instability when a sinusoidally varying torque is applied to the spacecraft for a range of forcing amplitudes and frequencies. Such a torque, in practice, may arise under malfunction of the control system or from an unbalanced rotor. Chaotic instabilities arising from these torques could introduce uncertainties and irregularities into a spacecraft's attitude motion and, consequently, could have disastrous effects on its operation. The two control methods, recursive proportional feedback and continuous delayed feedback, are recently developed techniques for control of chaotic motion in dynamic systems. Each technique is outlined and the effectiveness on this model compared and contrasted. Numerical simulations are performed, and the results are studied by means of time history, phase space, Poincaré map, Lyapunov characteristic exponents, and bifurcation diagrams.

Introduction

THE present paper investigates control of chaotic instability behavior in the attitude dynamics of dual-spin spacecraft with internal energy dissipation. Recently, many investigations of the stability and dynamics of similar configurations have been performed after abnormalities in spacecraft were found in practice. For instance, many researchers[1–3] have found parametric fluctuations resulting from structural imperfections in the attitude behavior of a dual-spin spacecraft. Recent attention has also been concentrated on investigating chaotic instabilities that can arise in a spacecraft system. Holmes and Marsden,[4] Koiller,[5] and Gray et al.[6] have performed analyses on spacecraft configurations using Melnikov's method to show the existence of horseshoes for spinning motion about the intermediate moment of inertia axis. Piper and Kwatny[7] have also investigated a commonly used momentum exchange spacecraft attitude control configuration and have shown the existence of multiple limit cycles and strange attractors for a range of motor time constants. These results are of importance to spacecraft designers because any instabilities in the attitude dynamics of a spacecraft could have disastrous effects on its normal operation. For example, chaotic motion in the attitude motion of a communication satellite would be seriously detrimental to the high pointing accuracies required by antennas providing the desired coverage on the Earth's surface. Thus, it is prudent for designers to avoid the regions of chaotic instability via parameter design; however, a successful control methodology would allow designers to use spacecraft parameters (desired for other requirements) that would normally render the spacecraft susceptible to chaotic instabilities. This paper extends the understanding of this form of instabilities in spacecraft systems by investigating possible control strategies to quench these instabilities.

In the recent past, a vast array of different control techniques have been employed successfully to suppress or manipulate chaotic instabilities. Lindner and Ditto[8] and Blazejczyk et al.[9] present a comprehensive review of these techniques. The present research uses two methods for the control of chaotic vibrations in a simplified model of a dual-spin spacecraft. The first method, recursive proportional feedback (RPF) derived by Rollins et al.,[10] is an extension of the occasional proportional feedback (OPF)[11,12] technique. The second technique is a continuous delayed feedback method devised by Pyragas.[13] Both of these methods are derived from the renowned model-independent technique proposed by Ott, Grebogi, and Yorke (OGY) (see Ref. 8) and require no prior knowledge of the system dynamics. Hunt[11] and Roy et al.[12] give two examples of the employment of the OPF method in experimental systems and Parmananda et al.[14] has used the RPF method to control the dissolution of the anode in an electrochemical cell.

For the purpose of the present analysis, a simple model of dual-spin spacecraft with an axial nutational damper is chosen, and no linearization of the equations of motion has been performed. An axial damper was chosen over a circumferential because of its effectiveness in operation for small nutation angles as found by Cochran and Thompson.[15] The problem involves the study of a body with internal moving parts such that the resulting dynamics involves a coupling of the motions of the damper mass and the angular rotations of the platform and rotor of the spacecraft. Chaotic motion has previously been found in this simplified model by Meehan and Asokanthan[16] when the rotor is subjected to a periodically varying torque. Such a torque, in practice, may arise in a dual-spin spacecraft under malfunction of the control system, causing periodic rotor driver fluctuations. A similar situation may also arise in a dual-spin spacecraft during spin-up of an unbalanced rotor or from vibrations in appendages. Two control methods will be applied to the system, under the conditions causing chaotic motion, to eliminate instabilities.

This paper first gives a simplified description and formulation of the equations of motion governing the dynamics of the system. A summary of the results obtained, describing the presence of chaotic instabilities, is then provided. Also, an outline of each control method and its design implementation is presented. Numerical simulation results are shown and the effectiveness of each control method on this model is compared and contrasted.

Equations of Motion and Stability Analysis

The system under investigation consists of a dual-spin spacecraft in the form of an axisymmetric rotor attached to an asymmetric platform that contains an axial nutational damper that is modeled by a spring–mass–dashpot as illustrated in Fig. 1. When the translational motion of the spacecraft is disregarded, the degrees of freedom of the system associated with the attitude motion are z, θ_x, θ_y, θ_z, and θ_r, which describe the displacement of the damper mass, three axis rotations of the system about the body-fixed frame of reference $Axyz$, and rotation of the rotor relative to the platform, respectively. The damper is centred on the body-fixed x axis and has a point mass of m that moves along an axis parallel to the z axis at a distance b from A. The spring constant is k, and the dashpot has damping constant c. The rotor is centered on the body-fixed z axis and is permitted to rotate about this axis only. The system rotates about its center of

Received 29 June 2000; revision received 2 July 2001; accepted for publication 22 July 2001.

*Lecturer, Department of Mechanical Engineering.
†Senior Lecturer, Department of Mechanical Engineering.

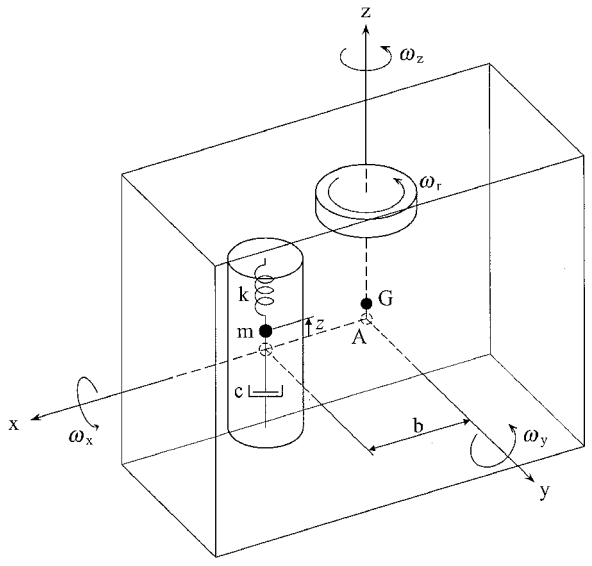

Fig. 1 Dual-spin spacecraft with an axial nutational damper.

mass at point G, which coincides with A when $z=0$. The system (including rotor and platform) is considered to have a total mass m_T and principal moments of inertia I_x, I_y, I_z when $z=0$. Note that the position of A with respect to the motionless center of mass G and the instantaneous principal moments of inertia of the system about A vary with the position of the damper mass. The rotor has a moment of inertia about the z axis I_r that is included in the system's principle moment of inertia I_z just described. The system is also considered to be subjected to a combination of internal torques T_r applied to the rotor bearing and composed of an excitational time-varying torque T_E and a control torque T_C such that $T_r = T_E + T_C$.

The equations of motion for the system have been obtained previously[16] in dimensional form using a generalization of the kinetic energy equation for any arbitrary frame of reference with arbitrary motion.[17] It is convenient to transform these equations to a nondimensional form by introducing the following dimensionless quantities

$$\tau = \Omega t, \qquad \mu = \frac{m}{m_T}, \qquad \hat{z} = \frac{(1-\mu)z}{b}$$

$$\left\{\left[\hat{\omega}_i = \frac{\omega_i}{\Omega}, \hat{I}_i = \frac{(1-\mu)I_i}{mb^2}\right]; i = x, y, z\right\}, \qquad \hat{c} = \frac{c}{m(1-\mu)\Omega}$$

$$\hat{k} = \frac{k}{m(1-\mu)\Omega^2}, \qquad \hat{T}_r = \frac{(1-\mu)T_r}{mb^2\Omega^2} \tag{1}$$

where Ω and τ denote the frequency of the time varying torque T_E and the nondimensional time, respectively. The quantity $\omega_i = \mathrm{d}\theta_i/\mathrm{d}t \equiv \dot{\theta}_i$ denotes the angular velocity about the body-fixed axes, $i = x, y, z$, and the carat superscript denotes a nondimensional parameter. By the use of Eqs. (1), the dimensionless equations of motion are derived as

$$\left(\hat{I}_x + \hat{z}^2\right)\hat{\omega}_x' - \hat{\omega}_y\hat{\omega}_z\left(\hat{I}_y - \hat{I}_z + \hat{z}^2\right) + 2\hat{\omega}_x\hat{z}\hat{z}' + \hat{I}_r\hat{\omega}_r\hat{\omega}_y - (\hat{\omega}_z' + \hat{\omega}_x\hat{\omega}_y)\hat{z} = 0 \tag{2}$$

$$\left(\hat{I}_y + \hat{z}^2\right)\hat{\omega}_y' - \hat{\omega}_x\hat{\omega}_z\left(\hat{I}_z - \hat{I}_x - \hat{z}^2\right) + 2\hat{\omega}_y\hat{z}\hat{z}' - \hat{I}_r\hat{\omega}_r\hat{\omega}_x + \left(\hat{\omega}_x^2 - \hat{\omega}_z^2\right)\hat{z} - \hat{z}'' = 0 \tag{3}$$

$$\hat{I}_z\hat{\omega}_z' - \hat{\omega}_x\hat{\omega}_y(\hat{I}_x - \hat{I}_y) + 2\hat{\omega}_x\hat{z}' + \hat{I}_r\hat{\omega}_r' + (\hat{\omega}_y\hat{\omega}_z - \hat{\omega}_x')\hat{z} = 0 \tag{4}$$

$$\hat{I}_r(\hat{\omega}_z' + \hat{\omega}_r') = \hat{T}_r \tag{5}$$

$$\hat{z}'' + c\hat{z}' + k\hat{z} - \left(\hat{\omega}_x^2 + \hat{\omega}_y^2\right)\hat{z} + \hat{\omega}_x\hat{\omega}_z - \hat{\omega}_y' = 0 \tag{6}$$

where the prime symbol denotes differentiation with respect to the dimensionless time τ. Equations (2–4) are the simplified set of Euler's equations representing the dynamics of a dual-spin spacecraft with an axial nutational damper. Equation (5) describes the angular acceleration-torque balance governing the relative motion of the rotor, and Eq. (7) represents the acceleration-force balance of the spring–mass–damper system. Note that the system described by Eqs. (2–6) is of order seven if $\hat{T}_r$ is assumed to vary periodically with time, and state equations described by $\hat{\theta}_i' = \hat{\omega}_i$ are trivial. Also note that Eqs. (2–4) and (6) are coupled through nonlinear terms resulting from the dynamic effects of the damper point mass and gyroscopic motion.

The stability analysis of this system has been performed previously by Meehan and Asokanthan.[16] By the setting of $[\hat{z}'\ \hat{z}''\ \hat{\omega}_x'\ \hat{\omega}_y'\ \hat{\omega}_z'\ \hat{\omega}_r']^T = [0\ 0\ 0\ 0\ 0\ 0]^T$ and $\hat{T}_r = 0$ in Eqs. (2–6) and solving, four equilibrium states were obtained.[16] Chaotic motion has previously been shown to arise[16,18] in the region in state space close to two of these equilibrium states under the influence of internal excitational torques. For the purpose of the present analysis, it was of interest to further investigate the behavior close to the equilibrium state described by

$$\hat{z} = \bar{z}, \qquad \hat{\omega}_x = \bar{\omega}_x, \qquad \hat{\omega}_y = 0, \qquad \hat{\omega}_z = \bar{z}\left(\bar{\omega}_x^2 - \hat{k}\right)\Big/(\bar{\omega}_x)$$

$$\hat{\omega}_r = \bar{z}\left\{\left(\bar{\omega}_x^2 - \hat{k}\right)\left[(\hat{I}_x - \hat{I}_z)\bar{\omega}_x^2 + \hat{k}\bar{z}^2\right] + \bar{\omega}_x^4\right\}\Big/\left(\hat{I}_r\bar{\omega}_x^3\right) \tag{7}$$

where $\bar{\omega}_x$, $\bar{\omega}_y$, $\bar{\omega}_z$, $\bar{\omega}_r$, and $\bar{z}$ indicate values that would depend on the initial conditions of the problem. Note that the stability configuration of the system may be determined completely with knowledge of the angular momentum and initial energy of the system, allowing the equilibrium states to reduce to a finite number of possible critical points. Equation (7) may represent a condition close to that expected from a dual-spin satellite in normal operation under certain conditions.

For the purpose of local linear stability analysis, two spacecraft parameter configurations with inertia ratios similar to those expected of external rotor and body-stabilized satellites were chosen. Typical inertia parameters for a Hughes external rotor satellite are $I_x = 505.708\ \mathrm{kg\cdot m^2}$, $I_y = 466.39\ \mathrm{kg\cdot m^2}$, $I_z = 471.814\ \mathrm{kg\cdot m^2}$, $I_r = 330.812\ \mathrm{kg\cdot m^2}$, and $\mu = 0.00554$. Kaplan[19] describes a vehicle with inertia ratios similar to those expected of future body-stabilized satellites of $I_x = 706\ \mathrm{kg\cdot m^2}$, $I_y = 645\ \mathrm{kg\cdot m^2}$, $I_z = 543\ \mathrm{kg\cdot m^2}$, $I_r = 0.08\ \mathrm{kg\cdot m^2}$, and $\mu = 0.01$. Other parameters chosen for both configurations are $m = 4$ kg, $b = 1$ m, $c = 0.4 \sim 2$ Ns/m, and $k = 8.7$ N/m. Angular momenta of 1905.7 and 1059.2 Nm · s were chosen for external rotor and body-stabilized satellite configurations, respectively. For each satellite parameter configuration, Meehan and Asokanthan[18] previously revealed that the equilibrium state (7) concerned was locally stable and, in particular, that for a given total system energy there exist at least two stable equilibrium points equidistant about the zero damper–mass position. It was also found that an external sinusoidal torque applied to the body about a perpendicular axis through A induces the system to jump chaotically between the two stable equilibrium points. The subsequent analysis will investigate the dynamic response of this system to a combination of torques $\hat{T}_r$ applied to the rotor bearing, composed of an excitational time-varying torque $\hat{T}_E$ and a control torque $\hat{T}_C$ such that $\hat{T}_r = \hat{T}_E + \hat{T}_C$.

Control Methods

The two control methods used in this paper are model-independent methods that exploit the universal characteristics of chaotic vibrations. Owing to this property, the methods employed are able to detect the presence of chaotic motion, switch on the control, and then switch it off once it is no longer required. For this system, the aim is to stabilize the desired state $[\hat{z}\ \hat{z}'\ \hat{\omega}_x\ \hat{\omega}_y\ \hat{\omega}_z\ \hat{\omega}_r]^T = [0\ 0\ 0\ 0\ \bar{\omega}_z\ \omega_{\mathrm{ref}}]^T$ that physically corresponds to the desired operation conditions for a satellite of constant rotation rates of platform and rotor with no nutation or precession. For simplicity in design of the control mechanism, the angular velocity of the rotor of the spacecraft $\hat{\omega}_r$ is chosen as the sensor variable, and the control actuator is considered to be a torque applied to the rotor bearing of the spacecraft $\hat{T}_C$. Such a control torque could be considered to be applied from the momentum wheel (or rotor)

spin-up motor in a bias momentum (or dual-spin) satellite. Thus, when the controlled system is being perturbed by an excitational periodically varying torque, it is considered to have a combination of applied torques $\hat{T}_r = \hat{T}_E + \hat{T}_C$ to the rotor bearing. Because of practical constraints, a torque limitation value of $T_{\max}$ is chosen for the control actuator.

Continuous Delayed Feedback Control

The first control method implemented on the present model was first proposed by Pyragas[13] as a method of time-continuous control. This method is based on the construction of a special form of a time-continuous perturbation that does not change the form of a desired unstable periodic orbit or fixed point. The control may be applied to any number of the system state-space equations in the form

$$\dot{\boldsymbol{X}} = \boldsymbol{F}(\boldsymbol{X}, p) + \hat{\boldsymbol{u}}_i C(\tau) \tag{8}$$

where $\dot{\boldsymbol{X}} = \boldsymbol{F}(\boldsymbol{X}, p)$ represents the state-space equations of motion, $\hat{\boldsymbol{u}}_i$ is a unit vector in the direction of the ith variable, and the control signal is sensitive to the ith variable in the form

$$C(\tau) = K[x_i(\tau - \Delta) - x_i(\tau)] \tag{9}$$

where Δ is the delay time and x_i is the ith variable. Note that $C(\tau) = 0$ when $x_i(\tau - \Delta) = x_i(\tau)$. This occurs when the system is settled on a limit cycle of period Δ. Control design is performed, in practice, simply by adjustment of the delay Δ to the period of the desired unstable periodic orbit and weight K of the feedback.

For the present model, a suitable choice for control parameters is $x_i \equiv \hat{\omega}$ such that after introducing a torque limitation $T_{\max}$, the controller law may be given by

$$\hat{T}_C(\tau) = \begin{Bmatrix} C(\tau), |\hat{T}_C(\tau)| < T_{\max} \\ T_{\max}, \hat{T}_C(\tau) > T_{\max} \\ -T_{\max}, \hat{T}_C(\tau) < -T_{\max} \end{Bmatrix}$$

$$C(\tau) = K[\hat{\omega}_r(\tau - \Delta) - \hat{\omega}_r(\tau)] \tag{10}$$

The block diagram that illustrates this form of control is seen in Fig. 2a. For the present model the aim is to stabilize a fixed point so that in practice the delay Δ is chosen to be smaller than the forcing period.

RPF Control

The second method, RPF control, is an extension of the OPF technique[11]. This method has been derived from the renowned technique proposed by OGY (see Ref. 8), which is model independent and goal oriented. Like the OPF method, the RPF is useful in highly dissipative systems where dynamics exhibit a nearly one-dimensional return map. RPF has an extra derivativelike term as compared to OPF that adds greater stability for control. The method, however, can only be applied to discrete mappings of a dynamic system.

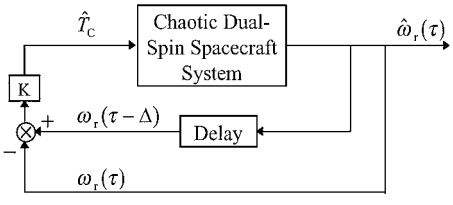

a) Continuous delayed feedback

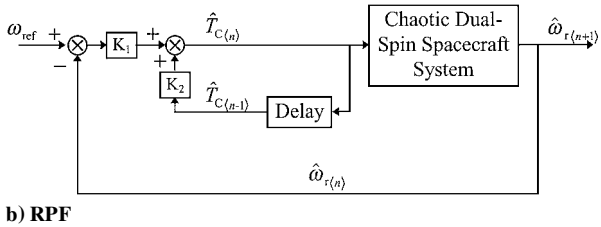

b) RPF

Fig. 2 Block diagram of control methods.

The control method provides small perturbations to a system parameter that is proportional to the error from the desired output of a sensor variable for the system. For a discrete mapping, the control law for the nth iterate is given by

$$\delta p_n = \begin{cases} K_1 \delta x_n + K_2 \delta p_{n-1} & |K_1 \delta x_n| \le \delta p_{\max} \\ 0 & |K_1 \delta x_n| > \delta p_{\max} \end{cases} \tag{11}$$

where δp_n, defined as $p_n - p_0$, is the relative control parameter perturbation and p_n and p_0 denote the control parameter for the nth iterate and the uncontrolled value of the control parameter, respectively. The relative sensor displacement δx_n from desired fixed point x_f is defined as $x_n - x_f$ where x_n signifies the sensor value at the nth iterate. Also, $|K_1 \delta x_n| \le \delta p_{\max}$ defines a region or window in phase space around the desired fixed point where linear approximation is valid, and $K_2 \delta p_{n-1}$ is a derivativelike term that can add stability and optimize the control method. Generally, the mapping frequency is chosen to be the same as an external forcing frequency or a natural frequency of the system. In practice, control design is performed via adjustment of the two feedback gains K_1 and K_2, as well as adjustment of the window size $\delta p_{\max}$.

For the present model, a suitable choice for control parameters is

$$p_n \equiv \hat{T}_{C\langle n\rangle}, \qquad p_0 \equiv 0, \qquad x_n \equiv \hat{\omega}_{r\langle n\rangle}, \qquad x_f \equiv \omega_{\text{ref}} \tag{12}$$

such that

$$\delta p_n \equiv \hat{T}_{C\langle n\rangle}, \qquad \delta x_n \equiv \hat{\omega}_{r\langle n\rangle} - \omega_{\text{ref}}, \qquad \delta p_{\max} \equiv T_{\max} \tag{13}$$

where subscript $\langle n\rangle$ is the nth map iterate. Therefore, the control law may be given by

$$\hat{T}_{C\langle n\rangle} = \begin{cases} K_1\left(\hat{\omega}_{r\langle n\rangle} - \omega_{\text{ref}}\right) + K_2 \hat{T}_{C\langle n-1\rangle} & \left|\hat{T}_{C\langle n\rangle}\right| \le T_{\max} \\ 0 & \left|\hat{T}_{C\langle n\rangle}\right| > T_{\max} \end{cases} \tag{14}$$

The block diagram of this system is seen in Fig. 2b. In practice, the control design is implemented on a continuous system by holding the control constant for each period of the excitation torque.

Numerical Simulations

The effect of the control methods on the chaotic dynamics of the system was investigated numerically by integrating Eqs. (2–7) while the system is subjected to a time-varying torque applied to the rotor. This rotor torque was described by $\hat{T}_r = \hat{T}_E + \hat{T}_C$, where $\hat{T}_E = \hat{T}_E \cos\tau$. The fourth order Runge–Kutta routine was used for numerical integration. To examine the effect of the control methods on nonlinear phenomena, tools such as time history, bifurcation diagrams of Poincaré maps, and Lyapunov exponents were employed using DYNAMICS, written by Nusse et al.[20]

The parameters and angular momenta of the dual-spin spacecraft with an axial nutational damper were chosen as described earlier in the stability analysis. An excitational rotor torque frequency of $\Omega = 0.02$ rad/s was applied to both configurations. For these parameters, it is noted from Meehan and Asokanthan[18] that the system has stable equilibrium points that are physically close about the states described by

$$[\hat{z} \quad \hat{z}' \quad \hat{\omega}_x \quad \hat{\omega}_y \quad \hat{\omega}_z \quad \hat{\omega}_r]^T = [0.01 \quad 0 \quad 0 \quad 0 \quad 179.95 \quad 31.39]^T \tag{15}$$

$$[\hat{z} \quad \hat{z}' \quad \hat{\omega}_x \quad \hat{\omega}_y \quad \hat{\omega}_z \quad \hat{\omega}_r]^T = [0.01 \quad 0 \quad 0 \quad 0 \quad 74.59 \quad 155.8 \times 10^3]^T \tag{16}$$

for the external rotor and body-stabilized satellite configurations, respectively. It was, therefore, of interest to investigate the dynamics of the system using these states as initial conditions. In a practical situation, these initial conditions described may be encountered during spin-up or spin-down of a satellite rotor.

First, the characteristic nonlinear phenomena in the open-loop system were investigated, primarily while varying the amplitude of the rotor excitational torque T_E. Figures 3a and 3b show typical bifurcation behavior of the equilibrium damper displacement z for an

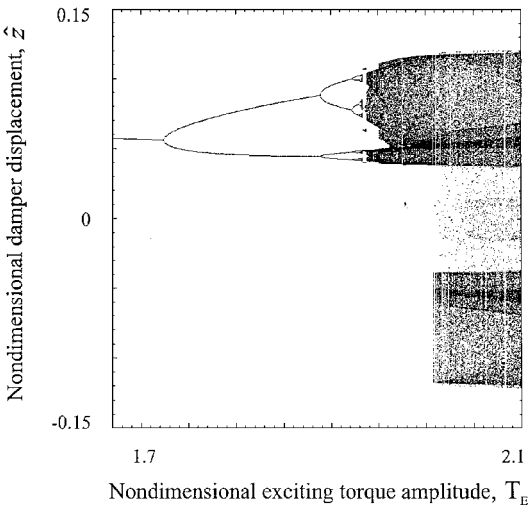

a) External rotor satellite

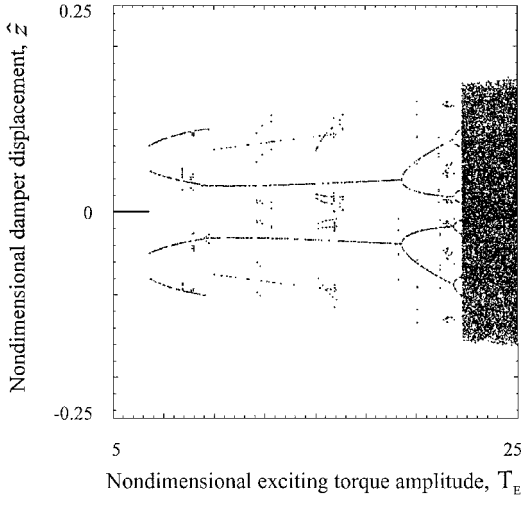

b) Body-stabilized satellite

Fig. 3 Bifurcation diagram showing chaotic motion.

increasing rotor excitational torque amplitude for the external rotor and body-stabilized satellite parameters, respectively. The evolution described in both Figs. (3a) and (3b) indicates a period doubling route to chaos. Chaotic motion is evident from the accumulation of bifurcations at torque amplitudes of 1.94 and 22 in Figs. 3a and 3b, respectively. Chaotic motion was also found for torque amplitudes of at least three orders of magnitude larger than the range indicated in Fig. 3a. The interaction of two attractors causing a larger chaotic attractor by a crisis phenomenon is also evident at a torque amplitude of 2.01. In Fig. 3b, the discontinuity in the bifurcation branching indicates the presence of more than one attractor with overlapping basins of attractions. Subsequently, it was of interest to investigate the effectiveness of the two control methods on the system while it is subjected to excitational torque amplitudes of $\hat{T}_E = 2.1$ and 24.8 for the external rotor and body-stabilized spacecraft configurations, respectively.

Figures 4–7 show the effect of each control method on the external rotor and body-stabilized spacecraft configurations by time histories of the control torque, damper mass position, and two angular velocities of the spacecraft. In each case the control loop is manually closed after a short interval as indicated on the diagrams so that a comparison of the open-loop and closed-loop systems can be made. The control torque limitation is also chosen in each case to be $T_{\max} = 500$.

Figures 4a–4d show the effect of applying the delayed feedback method to the external rotor configuration while it is behaving chaotically. Note that during the open-loop period, chaotic motion is manifested to a considerable extent in all of the dynamic variables of the spacecraft system such that the resultant attitude instability would be highly undesirable. Control of this attitude instability is achieved in the closed-loop period with the control parameters set at $K = 80$ and $\Delta = 0.1$. A large control torque is activated after the control loop is closed. The control is effective in eliminating the large amplitude instability in the damper–mass movement and angular velocities shown in Figs. 4b, 4c, and 4d, respectively. A similar effect is found in the other system variables not shown. The small residual oscillation in the rotor angular velocity seen in Fig. 4d arises because the control torque can not track the perodic excitational torque perfectly with a finite gain K.

Figures 5 show the effectiveness of the RPF control method for the same external rotor configuration and conditions. The open-loop and closed-loop dynamic behavior of the angular velocity $\hat{\omega}_x$ is shown in Fig. 5b and is indicative of the behavior of all of the other system variables. In this case, the control parameters were chosen to be $K_1 = 0.3$ and $K_2 = 0.1$. The desired reference angular velocity is chosen to be $\omega_{\text{ref}} = 50$. In comparison with the delayed feedback method, the steady-state control torque amplitude is negligible to achieve the same settling time for suppression of chaotic instability. However, it was noted that the amplitude of the residual oscillation in rotor angular velocity is larger. Note that optimization of control parameters may decrease this amplitude; however, the discreteness of the control method imposes a greater limitation in the reduction as compared to the continuous delayed feedback method. Also note that the control could not be achieved using reference angular velocities close to the initial angular velocities.

Figures 6 and 7 show similar results as Figs. 4 and 5 but for the body-stabilized configuration. In Fig. 6, control is achieved using the delayed feedback method by adjustment of the control parameters to $K = 0.1$ and $\Delta = 0.1$ periods. In Fig. 7 the desired reference angular velocity is chosen to be $\omega_{\text{ref}} = 190 \times 10^3$. Both methods are effective in eliminating the chaotic instability for the body-stabilized configuration. However, the settling time for the body-stabilized satellite is longer than that of the external rotor configuration.

To test the robustness of each control technique, the rotor excitational torque amplitude was varied, and a bifurcation diagram of the maximal Lyapunov exponent of the system was obtained for the open-loop and closed-loop cases. Figure 8 illustrates these results for the external rotor spacecraft configuration for the open-loop and closed-loop cases using continuous delayed feedback and the RPF method. For the open-loop case, chaotic motion, indicated by a positive maximal Lyapunov exponent, is present for excitational torque amplitudes $\hat{T}_E > 1.94$ as predicted in Fig. 3a. For the closed-loop results, the control parameters were chosen to be $K = 30$ and $\Delta = 0.25$ periods and $K_1 = 0.3$ and $K_2 = 0.1$ for the continuous delayed feedback and RPF method, respectively. The maximal Lyapunov exponent is reduced to zero for the same range of excitational torque amplitude as the open-loop case, indicating that the chaotic instability has been quenched in both cases. The zero maximal Lyapunov exponent obtained at the fixed point is due to the zero eigenvalue with eigenvector in the direction of the equilibrium lines $\bar{\omega}_z$ and $\bar{\omega}_r$. Bifurcation diagrams of time history confirmed that the desired equilibrium point was stabilized in each case.

Although both control methods were successful in eliminating the chaotic instabilities in the present model, for a range of rotor excitational torque amplitudes, a number of advantages and limitations were noticed. The delayed feedback method was seen to be more effective in suppressing the resultant oscillations in angular velocity. This may be attributed to the continuous nature of the method. The discrete nature of the RPF method could lead to some other serious limitations. As mentioned by Blazejczyk et. al.,[9] the method can only stabilize those periodic orbits whose maximal Lyapunov exponent is small compared to the reciprocal of the time interval between the parameter changes. Because the corrections of the control torque are rare and small, any fluctuation noise leads to occasional outbursts of the system into a region far from the desired periodic orbit. The RPF method was also unsuccessful in stabilizing desired angular velocities ω_{ref}, which were close to the initial value of $\hat{\omega}_r$. However, the RPF method is simple in design, requiring only one sensor and low control torques. The method also has the added flexibility over the delayed feedback method of control to any desired angular velocity ω_{ref}. In contrast, the final angular velocity is

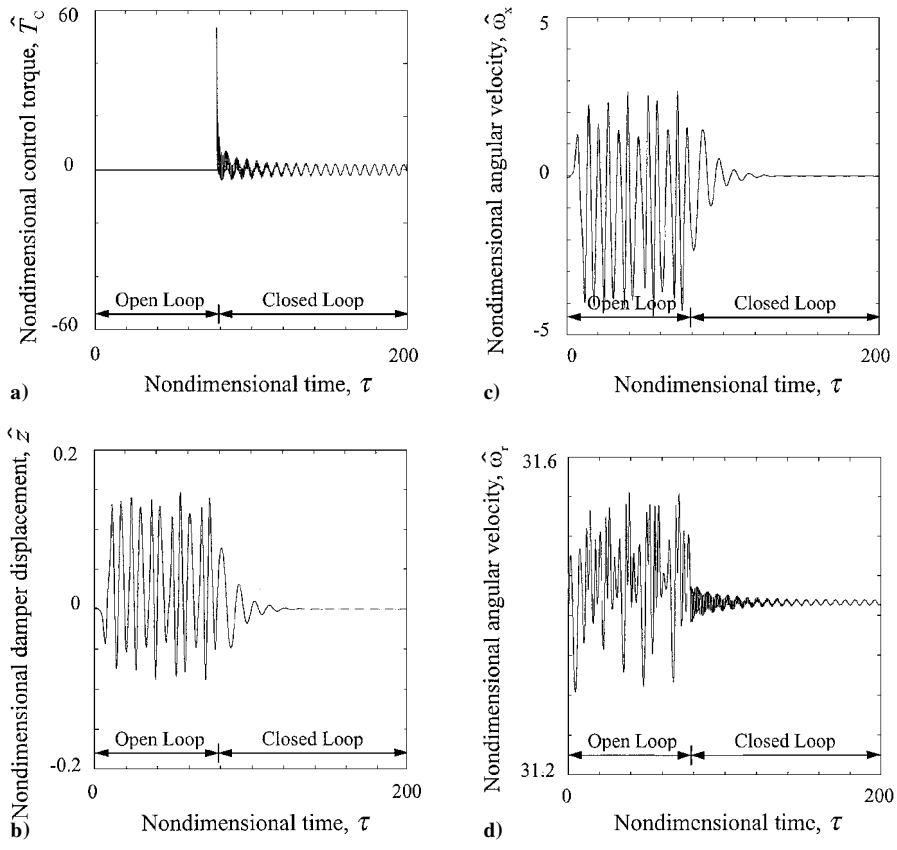

Fig. 4 Control using continuous delayed feedback for an external rotor satellite.

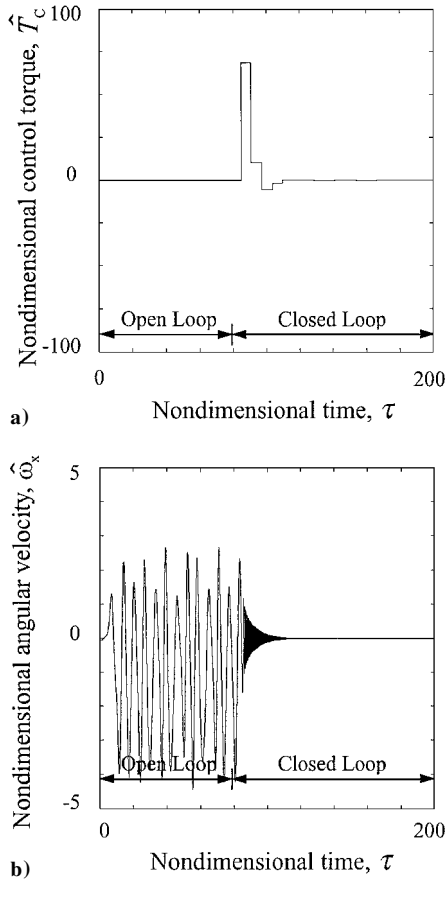

Fig. 5 Control using RPF for an external rotor satellite, $\omega_{ref} = 50$.

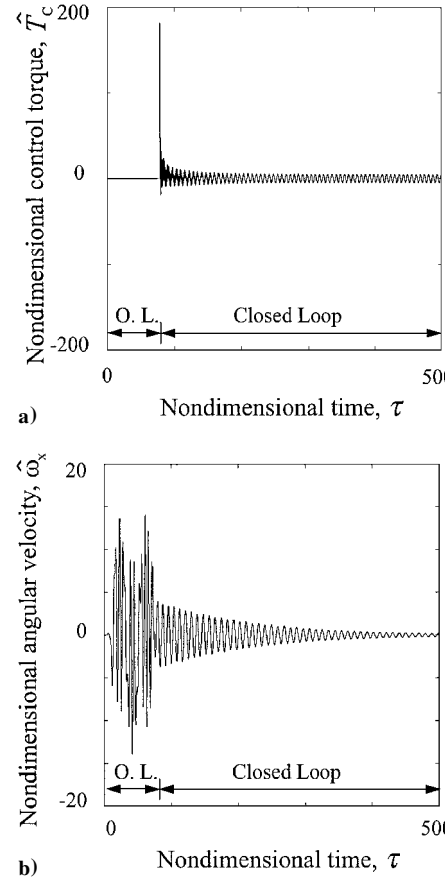

Fig. 6 Control using continuous delayed feedback for a body-stabilized satellite.

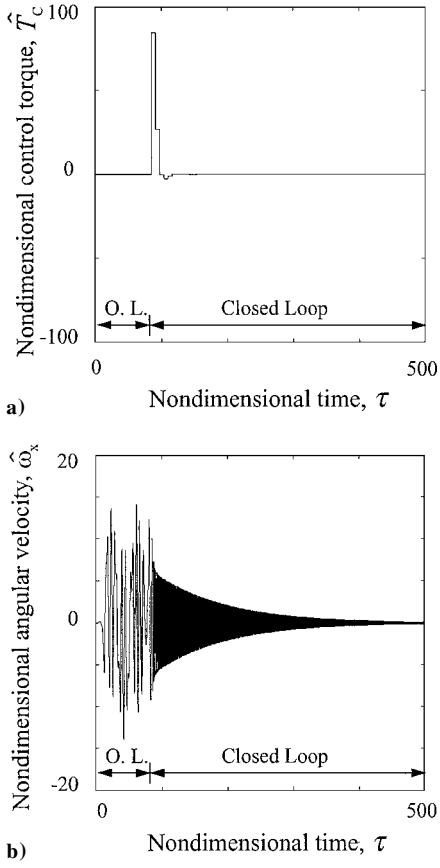

Fig. 7 Control using RPF for a body-stabilized satellite, $\omega_{ref} = 190 \times 10^3$.

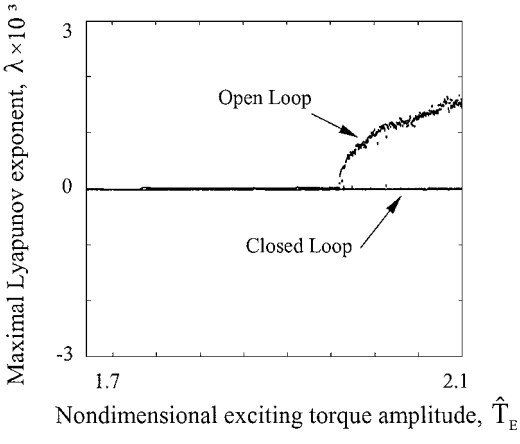

Fig. 8 Bifurcation diagrams of the maximum Lyapunov exponent showing control of chaotic motion.

determined by the total angular momentum of the system for the delayed feedback method. In practice, both techniques would be simple to implement on a spacecraft because they require no prior knowledge of the system dynamics.

Conclusions

Numerical simulations have shown the effectiveness of two control techniques in eliminating chaotic instabilities in a dual-spin spacecraft with internal energy dissipation when it is perturbed by a periodically varying torque applied to the rotor. Two typical spacecraft parameter configurations are investigated, and each is found to exhibit chaotic motion for a range of rotor torque perturbation amplitude and frequency. A similar situation, in practice, may arise in the platform of a dual-spin spacecraft under malfunction of the control system, during spin-up of an unbalanced rotor, or due to appendage vibrations. The control techniques are then successfully employed to eliminate the instability. The robustness of each technique is shown for a range of rotor excitational torque amplitudes. From a practical point of view, chaotic instabilities could introduce uncertainties and irregularities into a spacecraft's attitude and subsequently could have disastrous effects on its operation. It is, thus, important for spacecraft designers to be able to avoid these instabilities by employing the control techniques investigated in this paper. Each technique is outlined, and the effectiveness of this model compared and contrasted. In practice, both techniques would be simple to implement on a spacecraft because they require no prior knowledge of the system dynamics.

Acknowledgments

The authors greatly acknowledge the support of the members of the Applied Chaos Laboratory for their enlightening discussions and ideas while they were visiting the School of Physics at the Georgia Institute of Technology.

References

[1]Lukich, M. S., and Mingori, D. L., "Attitude Stability of Dual-Spin Spacecraft with Unsymmetrical Bodies," *Journal of Guidance, Control, and Dynamics*, Vol. 8, No. 1, 1985, pp. 110–117.

[2]Agrawal, B. N., "Attitude Stability of a Flexible Asymmetric Dual-Spin Spacecraft," *Proceedings of the AIAA Guidance and Control Conference*, AIAA, New York, 1983, pp. 120–127.

[3]Van Doorn, E., and Asokanthan, S. F., "Attitude Stability of an Asymmetric Spacecraft," *Proceedings of the IEAust Eighth National Space Engineering Symposium*, Inst. of Engineers, NCP 93/7, Barton, Australia, 1993, pp. 309–317.

[4]Holmes, P. J., and Marsden, J. E., "Horseshoes and Arnold Diffusion for Hamiltonian Systems on Lie Groups," *Indiana University Mathematics Journal*, Vol. 32, No. 2, 1983, pp. 273–309.

[5]Koiller, J., "A Mechanical System with a 'Wild' Horseshoe," *Journal of Mathematical Physics*, Vol. 25, No. 5, 1984, pp. 1599–1604.

[6]Gray, G. L., Kammer, D. C., and Dobson, I., "Detection of Chaotic Saddles in an Attitude Maneuver of a Spacecraft Containing a Viscous Damper," *Advances in the Astronautical Sciences*, Vol. 82, No. 1, 1993, pp. 167–184.

[7]Piper, G. E., and Kwatny, H. G., "Complicated Dynamics in Spacecraft Attitude Control Systems," *Journal of Guidance, Control, and Dynamics*, Vol. 15, No. 4, 1992, pp. 825–831.

[8]Lindner, J. F., and Ditto, W. L., "Removal, Suppression and Control of Chaos by Nonlinear Design," *Applied Mechanics Reviews*, Vol. 48, No. 12, Pt. 1,1995, pp. 795–808.

[9]Blazejczyk, B., Kapitaniak, T., Wojewoda, J., and Brindley, J., "Controlling Chaos in Mechanical Systems," *Applied Mechanics Reviews*, Vol. 46, No. 7, 1993, pp. 385–391.

[10]Rollins, R. W., Parmananda, P., and Sherard, P., "Controlling Chaos in Highly Dissipative Systems: A Simple Recursive Algorithm," *Physical Review E*, Vol. 47, No. 2, 1993, pp. R780–R783.

[11]Hunt, E. R., "Stabilising High Periodic Orbits in a Chaotic System: The Diode Resonator," *Physical Review Letters*, Vol. 67, No. 15, 1991, pp. 1953–1955.

[12]Roy, R., Murphy, T. W., Jr., Maier, T. D., Gills, Z., and Hunt, E. R., "Dynamical Control of a Chaotic Laser: Experimental Stabilisation of a Globally Coupled System," *Physical Review Letters*, Vol. 68, No. 9, 1992, pp. 1259–1262.

[13]Pyragas, K., "Continuous Control of Chaos by Self-Controlling Feedback," *Physics Letters A*, Vol. 170, No. 6, 1992, pp. 421–428.

[14]Parmananda, P., Sherard, P., Rollins, R. W., and Dewald, H. D., "Control of Chaos in an Electrochemical Cell," *Physical Review E*, Vol. 47, No. 5, 1993, pp. R3003–R3006.

[15]Cochran, J. E., Jr., and Thompson, J. A., "Nutation Dampers vs Precession Dampers for Asymmetric Spacecraft," *Journal of Guidance and Control*, Vol. 3, No. 1, 1980, pp. 22–28.

[16]Meehan, P. A., and Asokanthan, S. F., "Nonlinear Instabilities in a Dual-Spin Spacecraft with an Axial Nutational Damper," *Advances in the Astronautical Sciences*, Vol. 93, No. 2, 1996, pp. 905–923.

[17]Meehan, P. A., and Asokanthan, S. F., "Chaotic Motion in a Spinning Spacecraft with Circumferential Nutation Damper," *Nonlinear Dynamics*, Vol. 12, No. 1, 1997, pp. 69–87.

[18]Meehan, P. A., and Asokanthan, S. F., "Chaotic Motion in a Rotating Body with Internal Energy Dissipation," *Fields Institute Communications*, edited by W. H. Kliemann, W. F. Langford, and N. S. Namachchivaya, Vol. 9, American Mathematical Society, Providence, RI, 1996, pp. 175–202.

[19]Kaplan, M. H., *Modern Spacecraft Dynamics and Control*, Wiley, New York, 1976, Chap. 9.

[20]Nusse, H. E., Yorke, J. A., and Kostelich, E., *Dynamics: An Interactive Program for IBM-Compatible PCs and for UNIX*, Ver. 1, Springer-Verlag, New York, 1994.